

# Erraticity analysis of multiparticle production in $pp$ collisions at $\sqrt{s} = 2.76, 7 \text{ \& } 13 \text{ TeV}$

Presented by

**Tumpa Biswas**

**Cooch Behar Panchanan Barma University**

*tumpa.biswas.@cern.ch*

**Supervisor: Prof. Prabir Kumar Haldar**

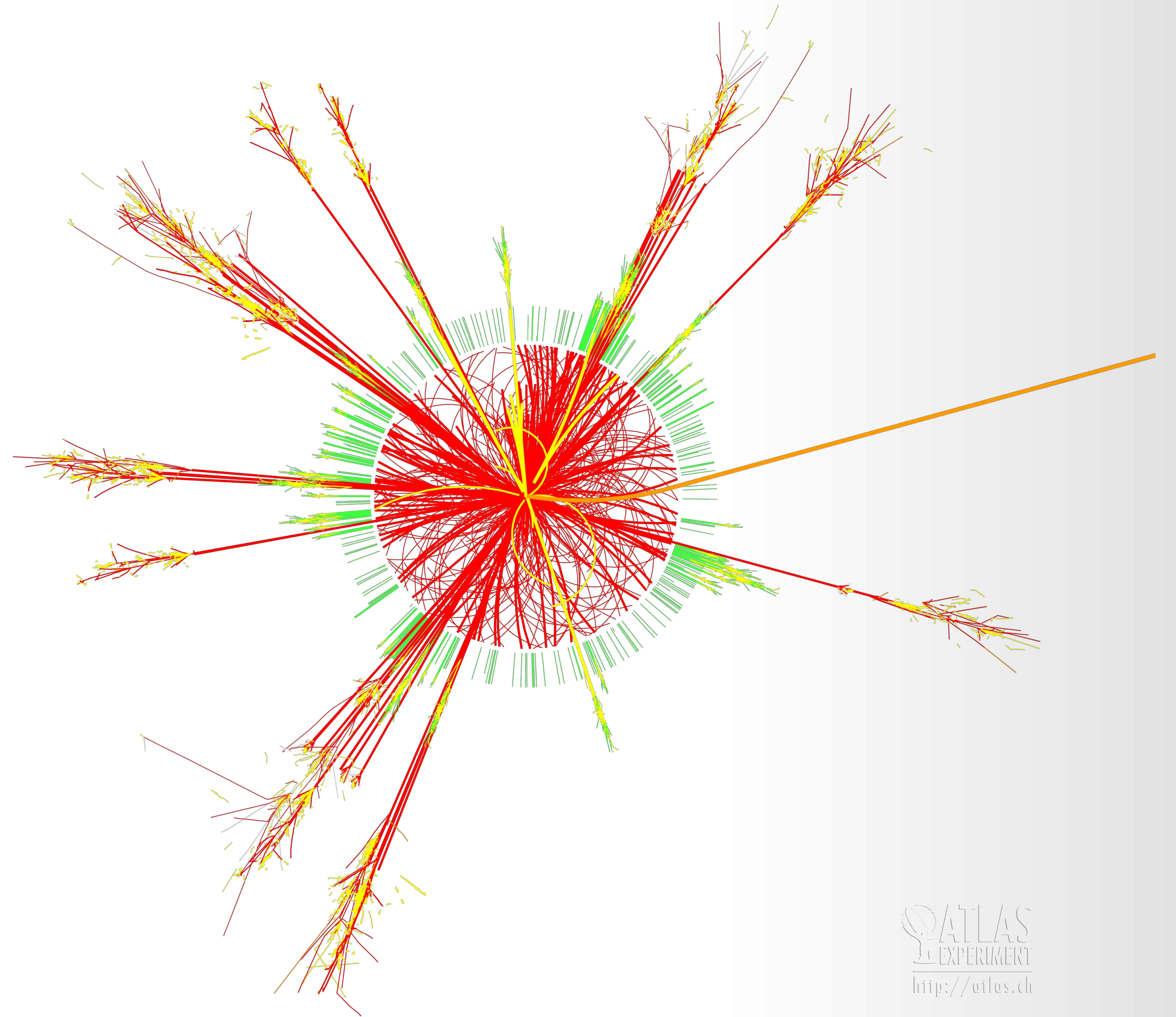


*ALICE-STAR India Collaboration Meeting, 2025*



# Overview

- Introduction
- Goal of the Study
- Data Description
- Methodology
- Results & discussion
- Conclusion



# Introduction

- Fluctuations in heavy-ion collisions can provide valuable insights into the formation of QGP. Significant fluctuation variables, such as energy fluctuation, charge fluctuation, multiplicity fluctuation and transverse momentum fluctuation, are considered so far.
- The density of emitted pions spectra fluctuates from bin to bin during the multi-pion production process, mainly due to spatial fluctuations. These fluctuations are also known as event space fluctuations as they differ from one interaction to another. When considering vertically averaged horizontal moments, only the spatial fluctuation is taken into account, while the event space fluctuation is ignored. On the other hand, when horizontally averaged vertical moments are considered, fluctuations from one event to the next are measured, but information about spatial fluctuation is lost. This results in the loss of information about the erratic nature of the multiparticle production processes.
- The fluctuations of spatial patterns from event to event are one of the significant properties of multi-pion production and it can reveal important insights about the underlying dynamics of particle production.
- To account for this issue, a new moment called “erratic” moments ( $C_{p,q}$ ) has been introduced by Hwa and Cao. These are the moments of factorial moment distributions and here both the spatial fluctuation and the event space fluctuation are taken into account; thus, it can provide a more comprehensive understanding of multiparticle production dynamics compared to factorial moments. These fluctuations are known to be associated with the system’s chaotic behavior.

# Goal of Study

In high-energy collisions, the produced particles prefer correlated emission and that leads to a spiky distribution. The reasons behind such a preference toward correlated emission may be (i) due to a second-order phase transition from QGP to normal hadronic matter; (ii) due to a random cascading effect in the space-time evolution of the collision process; (iii) due to some other collective phenomena like the formation of mini-jets, decay of giant resonances, emission Cerenkov gluons, etc.; and (or) (iv) due to a combination of any two or all of the above.

All the erraticity analyses reported so far have been performed at lower energies (compared to the LHC energies). Previously, it was believed that only high-energy heavy-ion collisions could produce QGP, while pp collisions served merely as baseline measurements to help us understand medium formation in nuclear collisions. However, recent advances in high-energy pp collisions have suggested that it is possible to form QGP droplets, particularly in high-multiplicity pp collisions, due to the observed heavy-ion like signatures in these events. In this article our aim is to carry out a detailed erraticity analysis of the same PYTHIA v8.3 generated datasets for  $\sqrt{s} = 2.76, 7 \text{ \& } 13 \text{ TeV}$ . It is worthwhile to mention that in this analysis, we have calculated  $\mu_{\tilde{q}}$ , which can offer valuable insights into the chaotic nature of the QCD branching process.

It is mandatory and interesting to note that PYTHIA 8.3 does not model a phase transition between quark-gluon plasma (QGP) and hadron gas. Instead, it employs phenomenological models to simulate the hadronization process, where partons transition into hadrons. Additionally, PYTHIA incorporates mechanisms like color reconnection and rope hadronization to account for phenomena such as strangeness enhancement and baryon production, which are observed in high-energy collisions and are indicative of QGP formation.

# Data Description

PYTHIA v8.3 is a general-purpose Monte-Carlo event generator mostly used to analyze proton–proton (pp) and proton–lepton collisions. Recent advancements in PYTHIA allow us to study high-energy collisions involving heavy nucleus, specifically pA and AA collisions. It provides a comprehensive framework for simulating fully exclusive final states that closely resemble those observed in collider experiments.

To generate our dataset, we enabled “softQCD on” and disabled “hardQCD off,” running simulations at various LHC energies. PYTHIA v8.3 is structured into three main levels. At the process level, the hard-scattering interaction takes place, producing transient resonances. This hard process is typically described using perturbative QCD, often involving only a small number of particles, particularly at high energies. Moving to the parton level, various shower models simulate both initial-state and final-state radiation, while additional effects, such as multiparton interactions (MPI), beam remnants and color reconnection (CR), contribute to the overall event structure.

In this study, we have considered datasets of  $10^6$  events for pp collisions at  $\sqrt{s} = 2.76, 7$  &  $13$  TeV energies.

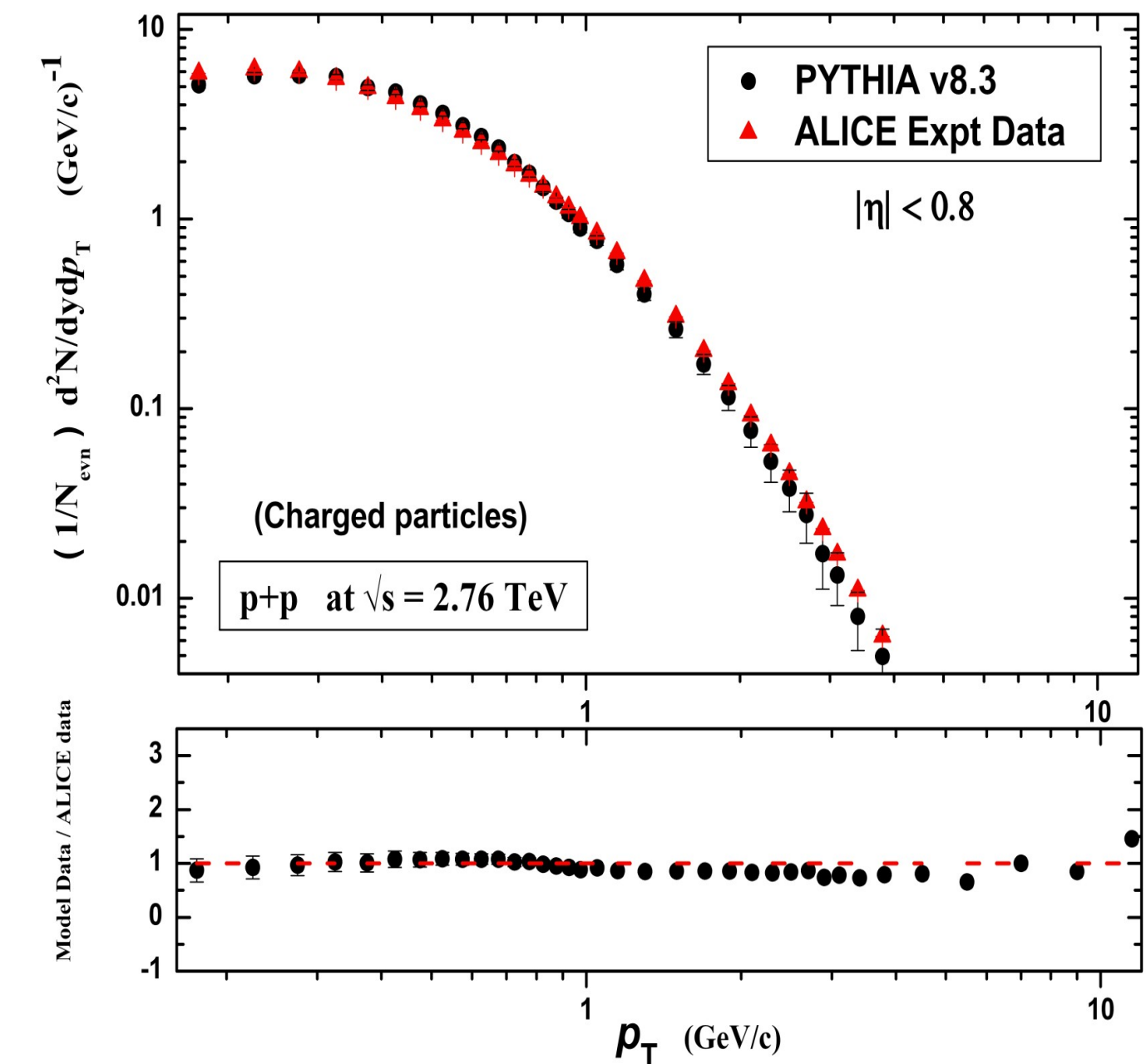


**Fig. 1: This graph compares the transverse momentum spectra and includes a ratio plot of charged particles between the minimum bias ALICE experimental dataset and the PYTHIA simulated dataset for pp interactions at  $\sqrt{s} = 2.76$  TeV**

# Methodology

The single-event factorial moment  $F_q^e$  of order  $q$  can be defined as,

$$F_q^e = \frac{\frac{1}{M} \sum_{m=1}^M n_m (n_m - 1) \cdots (n_m - q + 1)}{\left( \frac{1}{M} \sum_{m=1}^M n_m \right)^q}$$

where, the total pseudo-rapidity interval  $\delta\eta$  is subdivided into  $M$  bins of width  $\delta\eta = \eta/M$ .

A normalized moment  $\phi_q$  for an individual event can be defined as,

$$\phi_q = F_q^e / \langle F_q^e \rangle$$

$C_{p,q}$  moments defined as the vertically averaged  $p^{\text{th}}$ -order moment of  $\phi_q$

$$C_{p,q} = \langle \phi_q^p \rangle$$

An entropy-like quantity  $\Sigma_q$  defined as,

$$\Sigma_q = \langle \phi_q \ln \phi_q \rangle$$

$C_{p,q}$  follow a scaling law with phase space partition number  $M$  as,

$$C_{p,q} \propto M^{\psi(p,q)} : M \rightarrow \infty$$

$\psi(p,q)$  is called the “*erraticity index*.”

A generalized scaling law for  $\Sigma_q$  as follows,

$$\Sigma_q \propto \tilde{\mu}_q \ln f(M).$$

From the definitions of  $C_{p,q}$  and  $\Sigma_q$

$$\tilde{\mu}_q = \left. \frac{d}{dp} \tilde{\psi}(p,q) \right|_{p=1}.$$

$\tilde{\mu}_q$  is quite different from the entropy index  $\mu_q$ .

# Results & Discussion

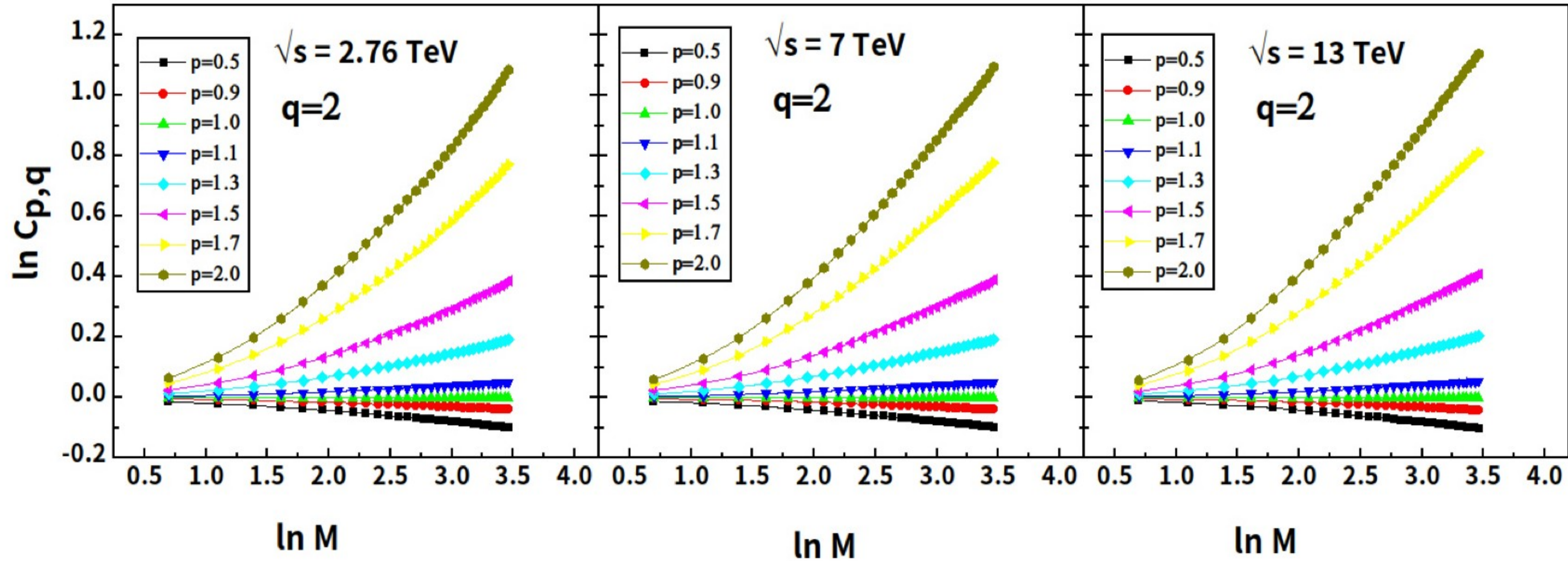


**Fig. 2:** Erraticity moments  $C_{p,q}$  plotted as functions of phase space partition number  $M$  for  $pp$  collisions at  $\sqrt{s} = 2.76, 7$  &  $13$  TeV.

This figure shows the variation of erraticity moments ( $C_{p,q}$ ) for  $q = 2$  over a wide range of  $p$  values (i.e.,  $p = 0.5, 0.9, 1.0, 1.1, 1.3, 1.5, 1.7$  &  $2.0$ ) against  $\ln M$  for  $\sqrt{s} = 2.76, 7$  &  $13$  TeV. From this figure it is evident that  $C_{p,q}$  exhibits a smooth but nonlinear increasing trend with increase in  $\ln M$  across the entire range.

# Results & Discussion

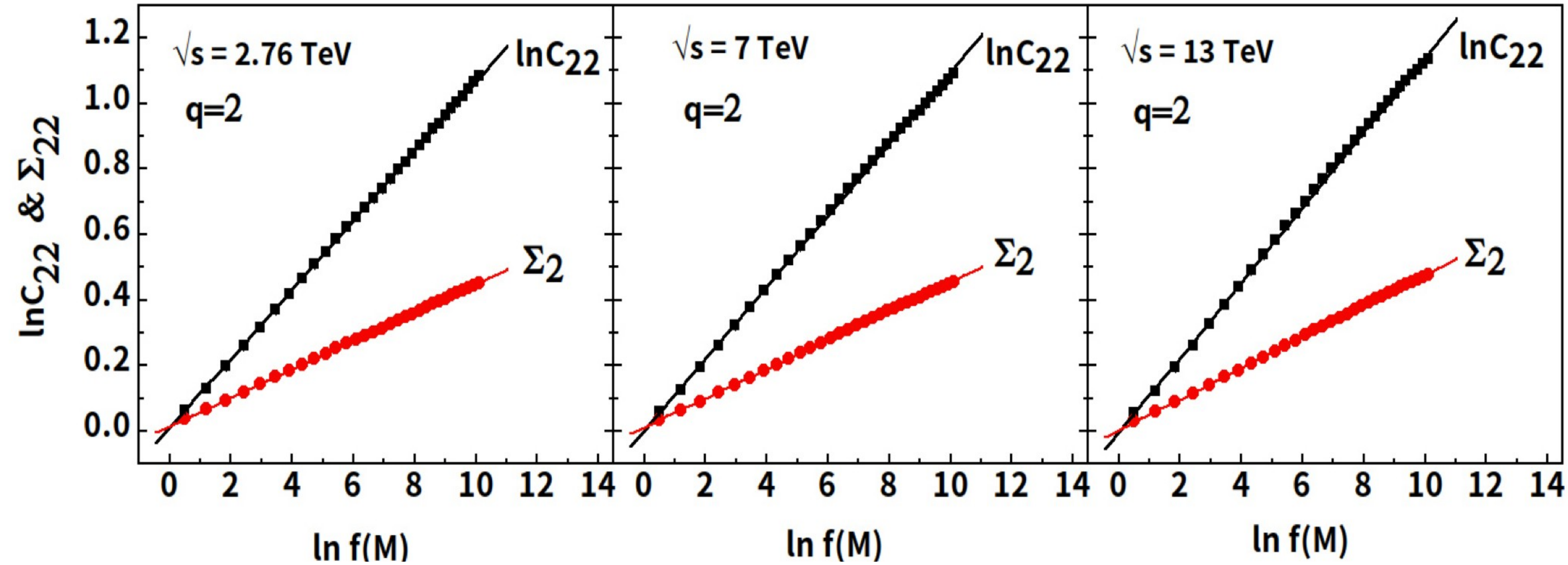


**Fig. 3:** Plot of  $\ln C_{2,2}$  and  $\Sigma_{2,2}$  with  $\ln f(M) = (\ln M)^b$  for  $pp$  collisions at  $\sqrt{s} = 2.76, 7$  &  $13$  TeV. The lines represent best linear fits to the data points.

Here we have assumed,  $\ln f(m)$  vs  $(\ln M)^b$  according to Cao and Hwa while taking  $b$  as a free parameter so that it can be adjusted from the linear fit of  $C_{2,2}$  versus  $\ln f(M)$  data and that plot is presented in Fig. 3 along with the best fitted straight line. The values of  $b$  are given in the second column of Table 1.

For all scenarios, the calculated values of Pearson's coefficient ( $R^2$ ) are found to be greater than 0.998 which indicates the existence of a strong correlation. Another parameter  $\tilde{\psi}_{(2,2)}$ , which is related to erraticity analysis, is also calculated from the slope of  $C_{2,2}$  versus  $\ln f(M)$  and the values of  $\tilde{\psi}_{(2,2)}$  are also provided in the third column of Table 1. In that same figure  $\Sigma_2$  is also plotted against  $\ln f(M)$ . Also the indices of  $\tilde{\mu}_2$  have been calculated from the linear relation between  $\Sigma_2$  and  $\ln f(M)$  using the  $b$  values which are already calculated from the best fit. The values of  $\tilde{\mu}_2$  are incorporated in the fourth column of Table 1.

**Table 1** Values of  $b$ ,  $\tilde{\psi}(2, 2)$  &  $\tilde{\mu}_2$  for PYTHIA in  $pp$  collisions at  $\sqrt{s} = 2.76, 7$  &  $13$  TeV

Energy (TeV)	$b$	$\tilde{\psi}(2, 2)$	$\tilde{\mu}_2$
2.76	1.86	$0.1055 \pm 0.0001$	$0.0433 \pm 0.0001$
7	1.86	$0.1092 \pm 0.0002$	$0.0443 \pm 0.0002$
13	1.82	$0.1143 \pm 0.0002$	$0.0475 \pm 0.0001$

# Results & Discussion

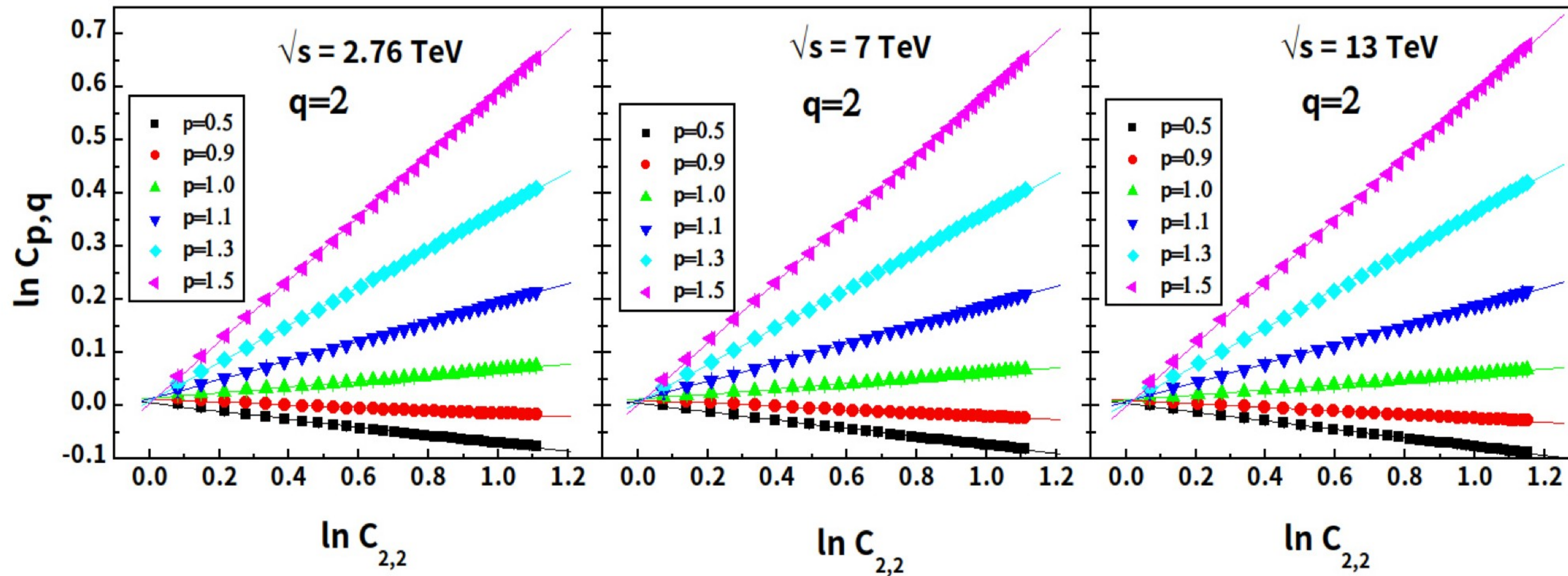


Fig. 4: Plot of  $\ln C_{p,q}$  with  $\ln C_{2,2}$ . The best fitted straight lines are shown for  $pp$  collisions at  $\sqrt{s} = 2.76, 7$  &  $13$  TeV

To calculate the erraticity parameters, we have replaced  $\ln f(M)$  with  $C_{2,2}$ . Therefore,

$$C_{p,q} \propto M^{\psi(p,q)} : M \rightarrow \infty \text{ is transformed to } C_{p,q} \propto (C_{2,2}) \times \tilde{\psi}_{(p,q)}$$

We find that for  $q = 2$ , the expected linear dependence of  $\ln C_{p,q}$  on  $\ln C_{2,2}$  is almost exact. For different values of  $p$ , the results are graphically presented in Fig. 4. For  $q > 2$ , the linear dependence is only approximate in the sense that it is valid only in the low- $M$  region.

# Results & Discussion

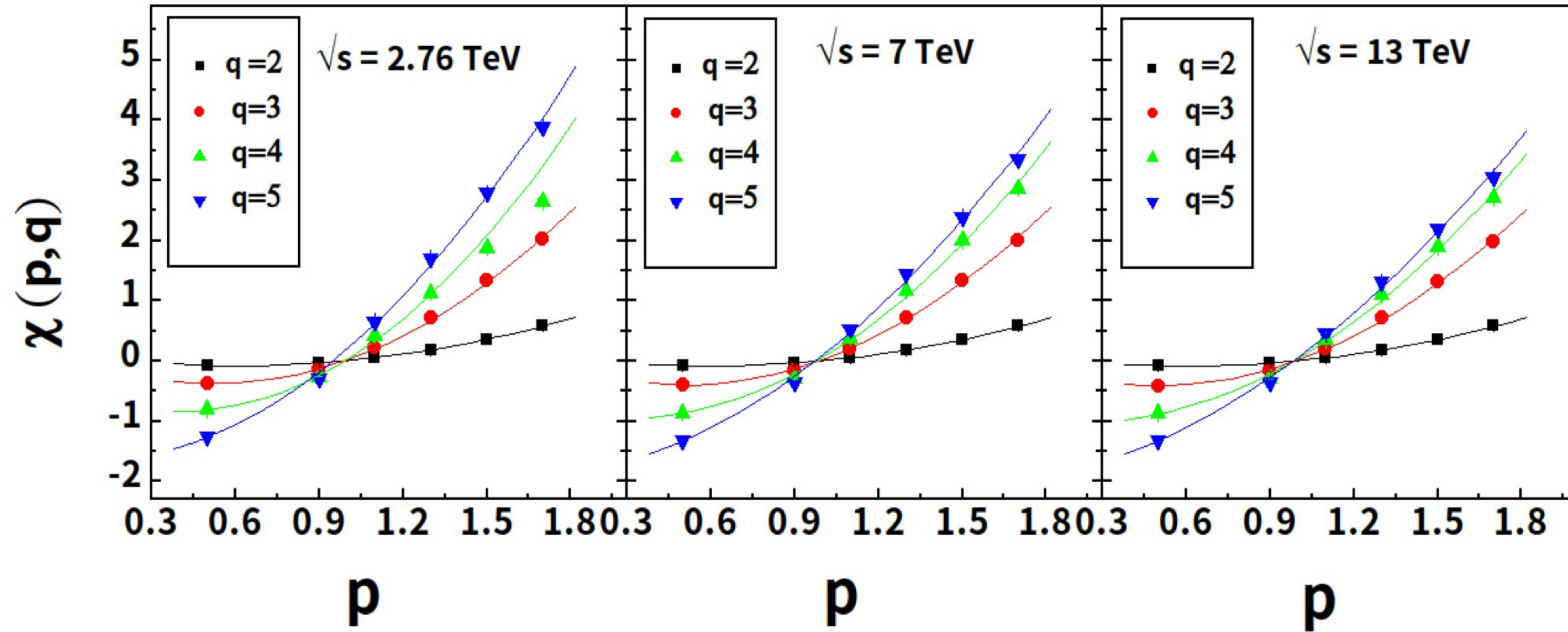


**Fig 5: Variation of  $\chi_{(p, q)}$  with  $p$  at  $\sqrt{s} = 2.76, 7$  &  $13$  TeV. The curves represent the best quadratic fits**

The effects of finite multiplicity and limited statistics are visible at large  $M$ . For  $q > 2$ , we have obtained  $\chi_{(p, q)}$  through a linear fit of the  $\ln C_{p, q}$  versus  $\ln C_{2, 2}$  data within a limited region of  $M(\leq 12)$ , where  $\ln C_{p, q}$  is found to behave systematically with  $\ln C_{2, 2}$ . Figure 5 shows the  $\chi_{(p, q)}$  versus  $p$  plots for different  $q$  values. The solid lines in these diagrams represent a quadratic function for a fixed  $q$  like,

$$\chi_{(p, q)} = a_2 p^2 + a_1 p + a_0$$

The solid curves in the diagrams represent this quadratic function.

# Results & Discussion

The entropy-like moments  $\Sigma_q$  for different  $q$  are also plotted against  $\ln M$  in Fig. 6. As expected, one can see that these moments are also not linearly varying with  $\ln M$  over its entire range. However, for all  $q$  the variation patterns look similar. Hence, in place of  $f(M)$  one can as well use  $\Sigma_2$  and make a plot of  $\Sigma_q$  against  $\Sigma_2$ , which is given in Fig. 7.

In each case, the slope parameters,

$$\omega_q = \frac{\partial}{\partial \Sigma_2} \Sigma_q$$

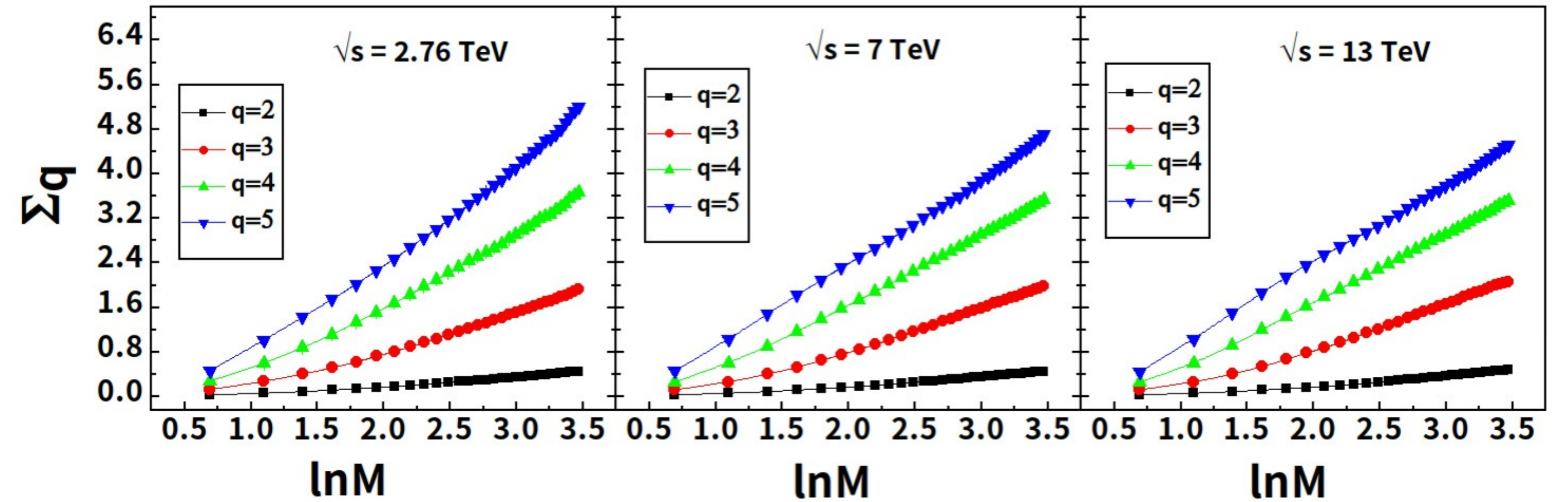


Fig 6: Plot of  $\Sigma_q$  with  $\ln M$ . The lines joining points are drawn to guide the eye.

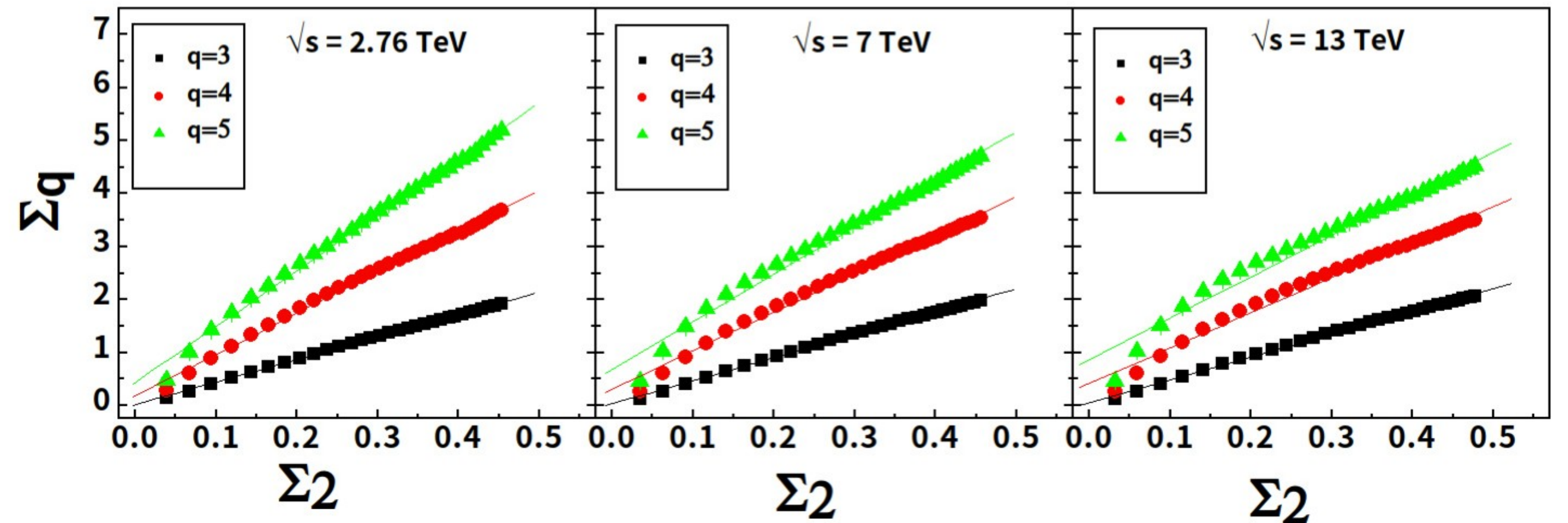


Fig 7: Plot of  $\Sigma_q$  against  $\Sigma_2$ . The lines represent the best linear fits to the data points.

# Results & Discussion

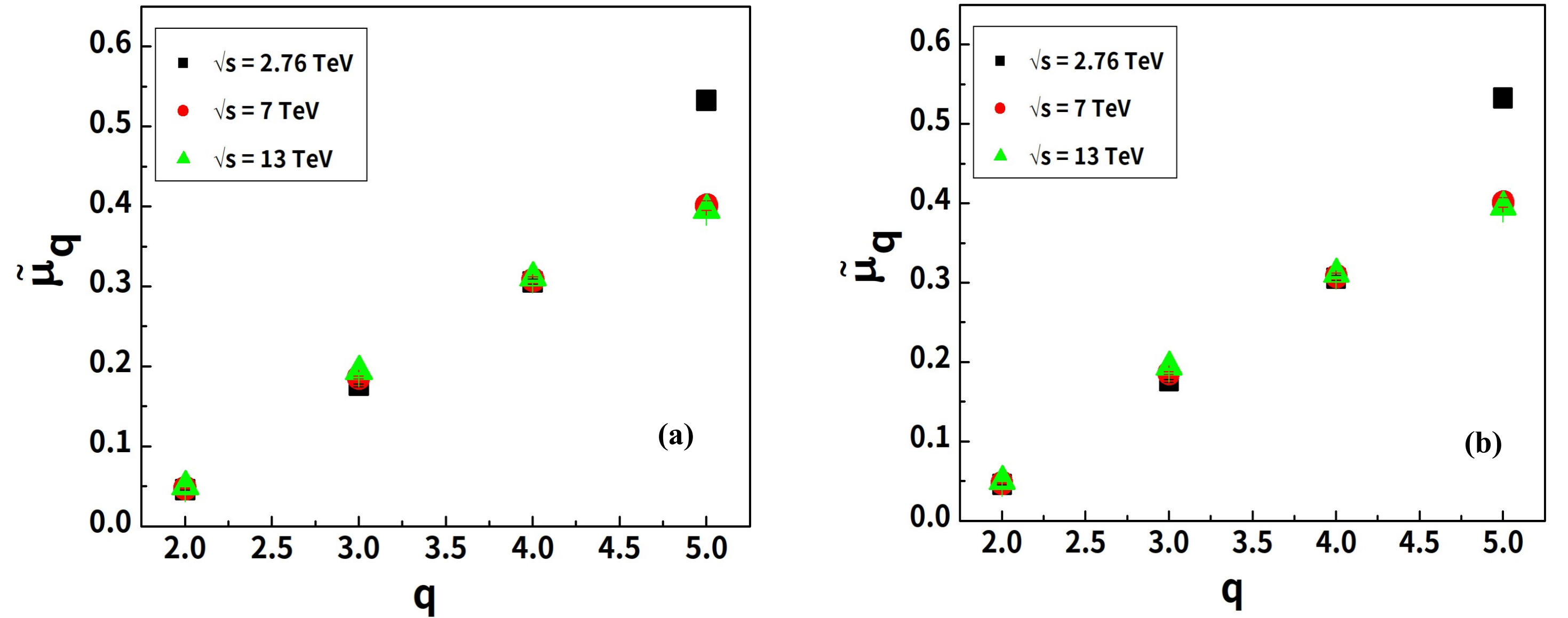
**Table 2** Erraticity parameters for  $pp$  collisions at  $\sqrt{s} = 2.76, 7$  &  $13$  TeV

Energy (TeV)	Order	$\chi'_q$	$\omega_q$	$\tilde{\mu}_q = \tilde{\psi}(2, 2) \chi'_q$	$\tilde{\mu}_q = \tilde{\mu}_2 \omega_q$
2.76	2	$0.4354 \pm 0.0066$	$4.2450 \pm 0.0286$	$0.0459 \pm 0.0007$	$0.1838 \pm 0.0017$
	3	$1.6698 \pm 0.0147$	$7.7740 \pm 0.0976$	$0.1762 \pm 0.0017$	$0.3366 \pm 0.0050$
	4	$2.8976 \pm 0.0276$	$10.5617 \pm 0.1422$	$0.3057 \pm 0.0032$	$0.4573 \pm 0.0072$
	5	$3.9955 \pm 0.0509$	$13.0404 \pm 0.1558$	$0.5327 \pm 0.0057$	$0.5646 \pm 0.0080$
7	2	$0.4356 \pm 0.0052$	$4.3479 \pm 0.0346$	$0.0476 \pm 0.0007$	$0.1926 \pm 0.0024$
	3	$1.7033 \pm 0.0156$	$7.2711 \pm 0.1297$	$0.1860 \pm 0.0020$	$0.3221 \pm 0.0072$
	4	$2.8185 \pm 0.0358$	$8.9745 \pm 0.2048$	$0.3078 \pm 0.0045$	$0.3976 \pm 0.0109$
	5	$3.6737 \pm 0.0564$	$10.3186 \pm 0.2447$	$0.4012 \pm 0.0062$	$0.4571 \pm 0.0129$
13	2	$0.4385 \pm 0.0051$	$4.3020 \pm 0.0408$	$0.0501 \pm 0.0007$	$0.2043 \pm 0.0024$
	3	$1.6978 \pm 0.0160$	$6.6803 \pm 0.1598$	$0.1941 \pm 0.0022$	$0.3173 \pm 0.0082$
	4	$2.7221 \pm 0.0373$	$7.8432 \pm 0.2463$	$0.3114 \pm 0.0048$	$0.3726 \pm 0.0125$
	5	$3.4623 \pm 0.0584$	$8.7866 \pm 0.2781$	$0.3957 \pm 0.0074$	$0.4174 \pm 0.0141$

All the erraticity parameters pertaining to this analysis of PYTHIA data, namely  $\chi_q$ ,  $\omega_q$  and two sets of  $\mu^{\sim}_q$  are presented in Table 1 and 2 for  $q = 2-5$ . Several observations can now be made regarding the erraticity behavior of our PYTHIA event sample. From Table 2, one can follow the entropy index  $\mu^{\sim}_q$  values calculated from both conditions are not similar for lower order of  $q$ , but as we go from lower to higher order, these values become quite similar.

# Results & Discussion

**Fig. 8:** Plot of the entropy index  $\mu_q$  against order number  $q$ , calculated using  $\psi_{(p,q)} \chi_q$  is presented in panel (a) and calculated using  $\mu_2 \omega_q$  is presented in panel (b) for  $pp$  collisions at  $\sqrt{s} = 2.76, 7, 13$ .



The measured values of  $C_{p,q}$  and  $\mu_q$  together give a collectively indicate a degree of chaoticity in a branching process, suggesting that QCD branching process is chaotic. For a better understanding of  $\mu_q$  values, we have plotted Fig. 8. From Fig. 8(a), it is visible that the values of  $\mu_q$  are almost similar for different orders of  $q$  except for  $q = 5$ . For  $q = 5$ , the values of  $\mu_q$  for  $\sqrt{s} = 7$  & 13 TeV are similar, but for  $\sqrt{s} = 2.76$ , TeV is much higher. From Fig. 8(b), only for  $q = 2$  & 3 the values of  $\mu_q$  look almost similar, but for other values of  $q$ , the values are higher for comparatively lower energies. One thing to note here that the values of  $\mu_q$  from figures [i.e., Fig. 8(a, b)] for  $\sqrt{s} = 2.76$  TeV of  $q = 5$  are quite higher respective to other energies. It is important to note that when the event multiplicity is low, the event factorial moments are unable to fully eliminate the statistical fluctuations caused by an insufficient number of particles. Therefore, in this study, the erratic behavior observed may not originate from dynamical origins but rather is primarily a result of trivial statistical fluctuations.

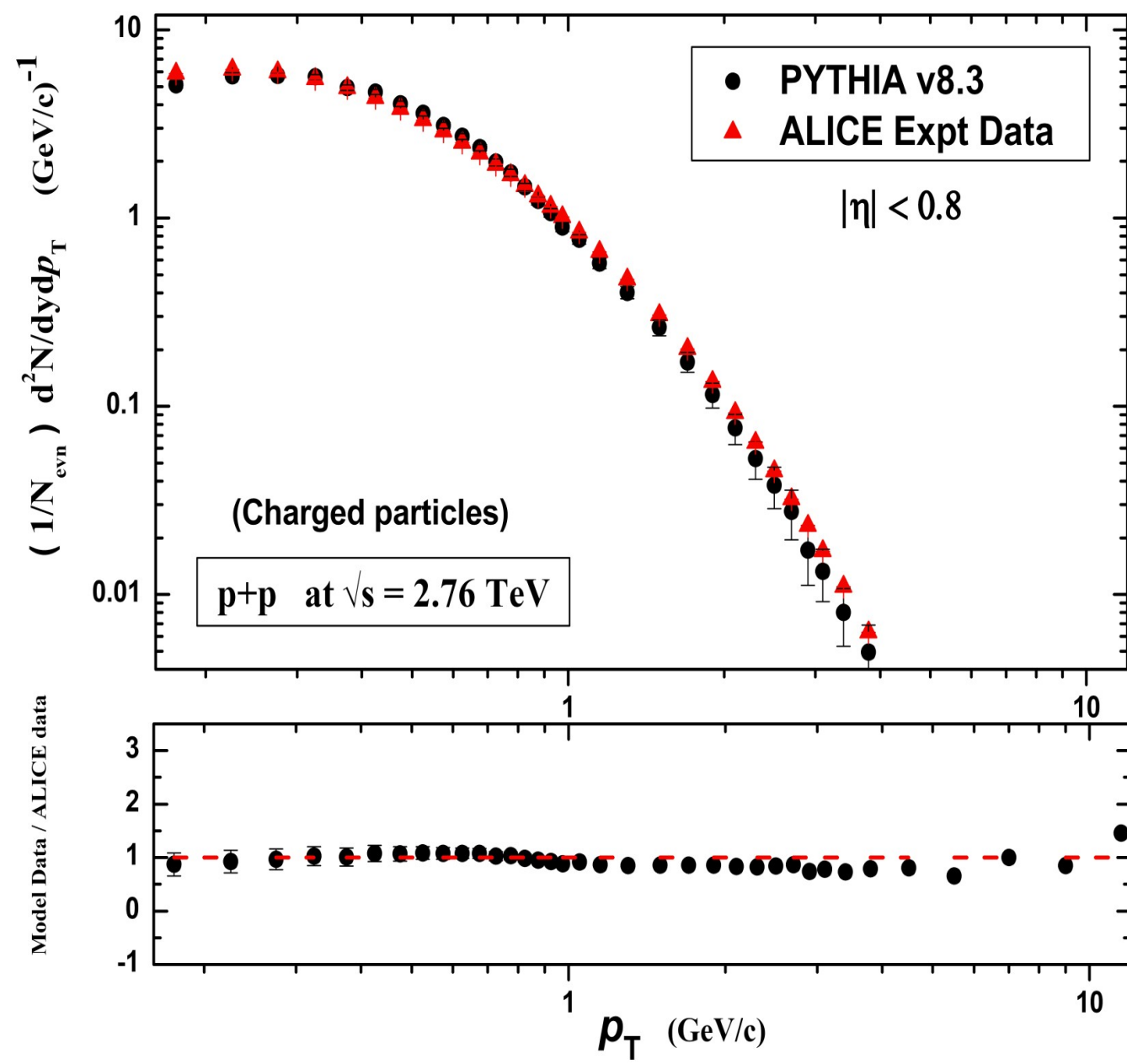
# Conclusions

The following critical observation can be made from the analysis.

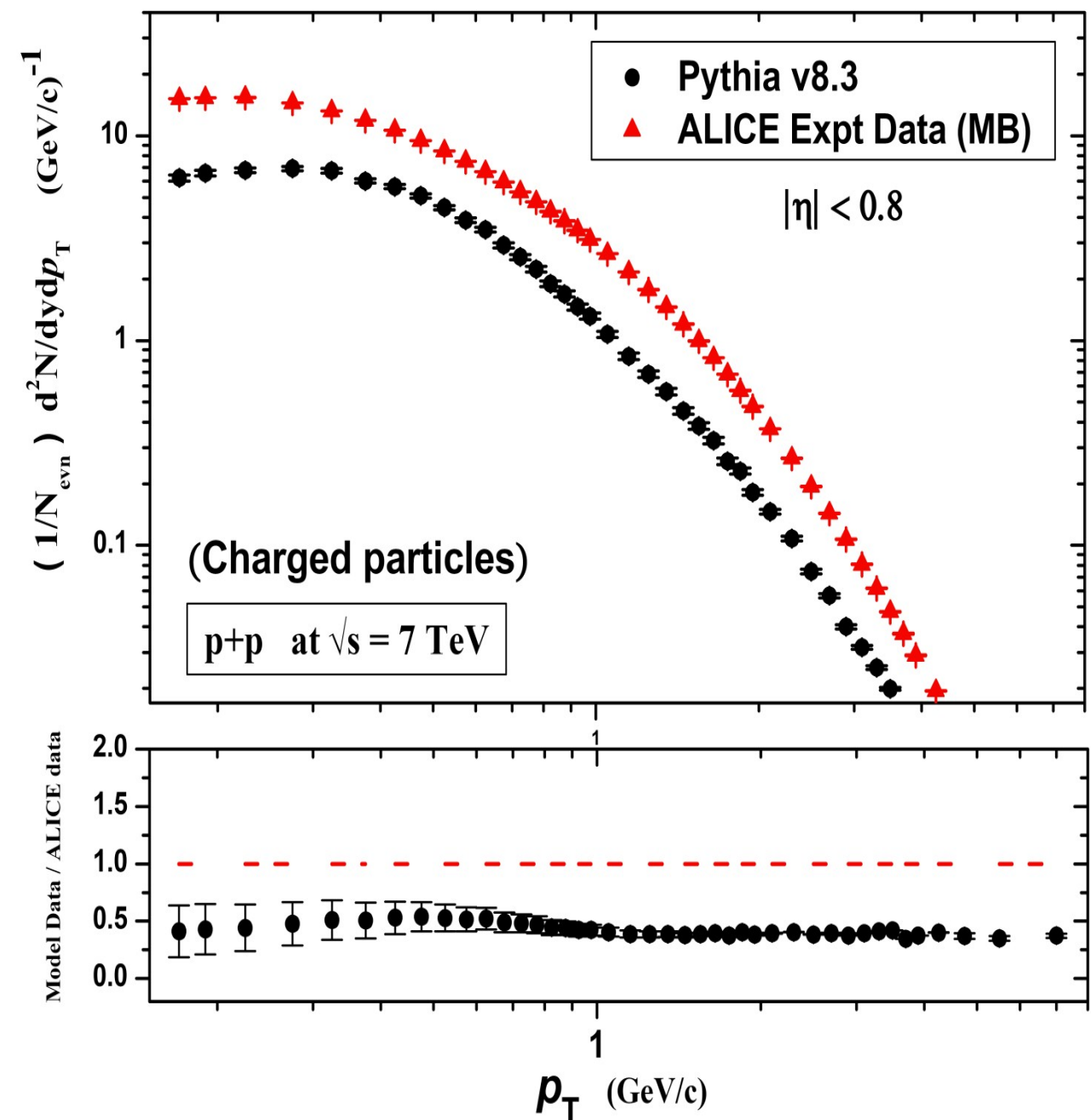
1. A substantial amount of event-to-event fluctuations of factorial moments are observed in the datasets. The fluctuations resulted in a power-law scaling variation of the erraticity moments  $C_{p,q}$  and  $q$ .
2. The erraticity moments are found to abide by a less strengthen generalized scaling law than the scaled factorial moment.
3. Most prominent fact that has been observed is that for higher orders of  $q$  at comparatively lower energies (i.e.,  $\sqrt{s} = 2.76$  TeV at  $q = 5$ ), the values of erraticity parameters are, respectively, higher than other energies which is quite interesting.
4. This study reports an increased entropy index, which may arise from various internal physics mechanisms considered in PYTHIA, such as MPI and CR, or may also be a result of statistical noise.
5. Additionally, the entropy index is associated with QCD branching, and its increasing value in case of PYTHIA-generated data suggests that the QCD branching process resembles chaotic behavior.
6. The multiparticle production in pp collisions is chaotic in nature. This analysis reports an increase in chaoticity with increase in energy ranges.



Backer



This graph compares the transverse momentum spectra and includes a ratio plot of charged particles between the minimum bias ALICE experimental dataset and the PYTHIA simulated dataset for pp interactions at  $\sqrt{s}$  2.76 TeV



This graph presents a comparison of the transverse momentum spectra from the ALICE experimental dataset and the dataset generated by PYTHIA. In panel (a) of Fig. 3, the graph shows the transverse momentum spectra of charged particles, including a ratio plot that compares the minimum bias ALICE experimental dataset with the PYTHIA simulated dataset for pp interactions at  $\sqrt{s}$  7 TeV.

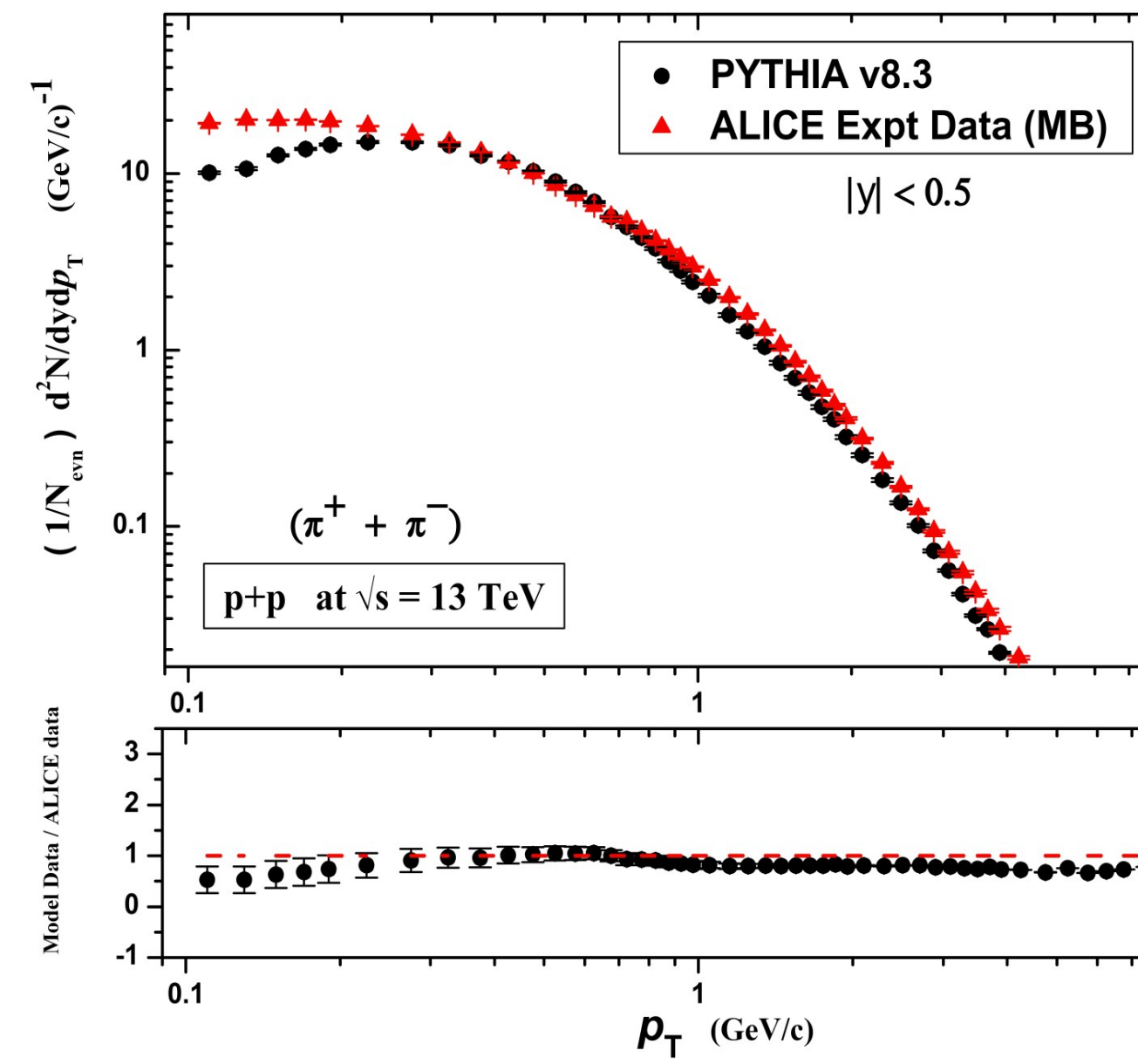
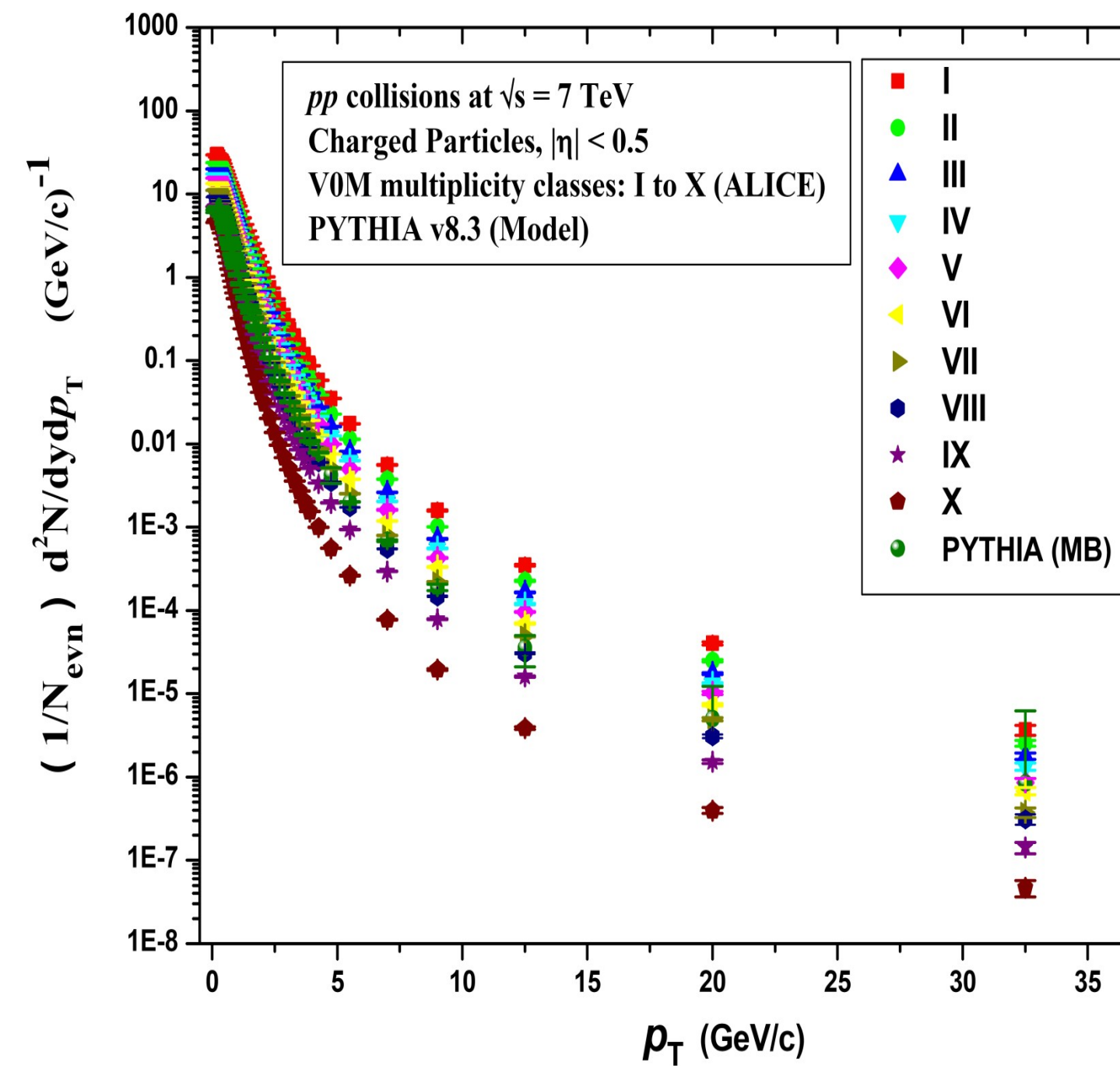


Fig. 2 This graph compares the transverse momentum spectra and includes a ratio plot of charged pions ( $\pi^+ + \pi^-$ ) between the minimum bias ALICE experimental dataset and the PYTHIA simulated dataset for pp interactions at  $\sqrt{s} = 13$  TeV



Panel (b) of Fig. 3 provides a further comparison of the transverse momentum spectra for the combined sum of positively and negatively charged particles across different event multiplicity classes (from I to X) in the ALICE experimental datasets.